Identification of features due to H_3^+ in the infrared spectrum of supernova 1987A

Steven Miller*, Jonathan Tennyson*, Stephen Lepp† & Alexander Dalgarno†

* Department of Physics and Astronomy, University College London, Gower Street, London WC1E 6BT, UK
† Harvard-Smithsonian Center for Astrophysics, 60 Garden Street, Cambridge, Massachusetts 02138, USA

THE molecular ion H_3^+ occupies a central position in theoretical models of interstellar chemistry[1,2]. It forms readily in hydrogen-rich interstellar gas clouds when ionized H_2 reacts with neutral H_2. The H_3^+ ion can then donate a proton to oxygen, carbon and other heavy atoms. From this beginning nearly 100 different interstellar molecules are formed, such as the reactive hydroxyl radical OH, neutral CO, ethanol, the linear polyacetylenes HC_xN and cyclic species such as cyclopropenylidene, C_3H_3. But in spite of a decade of searching[3,4], H_3^+ has eluded detection except in the hydrogen-rich atmosphere of Jupiter[5]. Here we present evidence for the presence of H_3^+ in the envelope of supernova 1987A, where it is produced by an unusual chemistry in which excited hydrogen atoms are the main source of molecule formation. Infrared spectra of SN1987A (ref. 6) in the first few hundred days after the explosion contain two previously unidentified peaks which we attribute to H_3^+. Chemical modelling produces quantities of H_3^+ consistent with the observed peak intensities, and also predicts significant amounts of HeH^+, which may be responsible for some weaker features in the spectra.

The infrared L-window spectra of supernova (SN) 1987A between 2.95 and 4.15 μm are dominated by three hydrogen recombination lines[6]. But from day 110 onwards, there are strong, hitherto unidentified, features at 3.409 (3.41) and 3.533 (3.53) μm. These are precisely the wavelengths at which H_3^+ announces its presence most strongly in Jupiter[7,8]. These features are clearest in the spectrum for day 192. Treating the mass of emitting H_3^+, M_e, the velocity width at half maximum, V_w, and the temperature, T_{exc}, as disposable parameters, we have fitted the two features to emission from H_3^+ using the observed frequencies and calculated transition probabilities[9,10] and an ortho-para ratio of 1.0. The background continuum was accommodated using a form similar to that of Meikle *et al.*[6] for the J, H and K windows:

$$B(\lambda) = a + b(\lambda - 3.60)^{-2.5} \quad (1)$$

where λ is the wavelength in micrometres. The fit produced values of $M_e = 5.1 \times 10^{-8}\ M_\odot$, $T_{exc} = 2{,}050$ K, $V_w = 3{,}200$ km s^{-1}, and $a = 0.0$ and $b = 0.6808$ in units of 10^{-8} erg s^{-1} cm^{-2} μm^{-1} (Fig. 1).

We have propagated the spectrum of H_3^+ obtained from our fitted values through the L window. For wavelengths longer than Pfund δ at 3.318 μm, the observed spectrum is entirely consistent with our fit, with features resulting from H_3^+ contributing to the observed intensity in regions other than those specifically fitted. But at shorter wavelengths we predict a strong feature at 3.2 μm and weaker peak centred on 3.02 μm, which are not observed. These wavelengths correspond to regions of strong atmospheric water absorption, however, which may account for the discrepancy between the calculated and observed spectra.

But there may also be other contributors to the spectra that would alter the H_3^+ parameters we have derived. In particular, Lucy *et al.*[11] have suggested that the 3.41-μm feature results from the 5^2S–4^2P^0 doublet of sodium. This close doublet cannot, however, account for the width of the 3.41-μm feature, and their interpretation encounters difficulties that can perhaps be resolved by the presence of another emitter. We can accommodate a contribution from a second emitter, such as sodium, by reducing the H_3^+ excitation temperature. In Fig. 2 we show the H_3^+ spectrum for $T_{exc} = 1{,}000$ K. Lowering T_{exc} has the additional advantage that the predicted feature at 3.2 μm is much weaker and the discrepancy between the computed and observed spectra around 3.02 μm is removed.

TABLE 1 H_3^+ and HeH^+ mass

Epoch (days)	H_3^+ ($M_\odot$)	HeH^+ ($M_\odot$)
100	8.8×10^{-8}	1.4×10^{-8}
150	1.2×10^{-7}	2.2×10^{-8}
200	1.1×10^{-7}	2.5×10^{-8}
250	8.3×10^{-8}	2.5×10^{-8}
300	5.3×10^{-8}	2.2×10^{-8}
350	3.3×10^{-8}	1.8×10^{-8}

The ejecta of SN1987A consist of an envelope almost entirely composed of hydrogen and helium, and an inner core region in which the heavier elements are to be found. Densities are low in the supernova envelope, and local thermodynamic equilibrium is unlikely to prevail. Accurate values for the total mass of H_3^+ will require a comprehensive study of the excitation conditions. But, given that the excitation temperature 1,000–2,000 K is similar to the kinetic temperature (which cannot exceed 3,000 K, as molecules are rapidly destroyed at temperatures higher than this), a total H_3^+ mass of $\sim 10^{-7}\ M_\odot$ is a reasonable estimate.

A mass of this order can be produced in the envelope of SN1987A by a chemistry initiated by the deposition of γ-rays. Recombination line profiles[12,13] show that hydrogen is not confined to the outer envelope of SN1987A but is mixed through the ejecta. In a pure hydrogen gas, H_3^+ is formed by the reaction

$$H_2^+ + H_2 \rightarrow H_3^+ + H \quad (2)$$

The H_2^+ ions are formed by radiative association, and the H_2 molecules by charge transfer from H to H_2^+ and by a negative ion sequence. In the supernova envelope, a large population

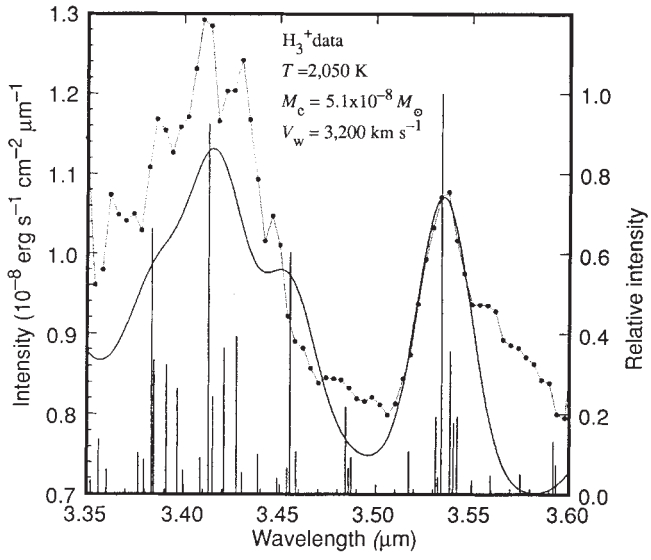

FIG. 1 Fit of the computed H_3^+ $\nu_2 \rightarrow 0$ spectrum (solid curve) to the L-window spectrum of SN1987A on day 192 (ref. 6) (filled circles) from 3.35 to 3.60 μm. Line positions and relative intensities of the individual H_3^+ transitions that blend to form the 3.41- and 3.53-μm features are shown. The 3.53-μm feature results from a blend of two R(2) and two R(3) transitions in the $\nu_2 \rightarrow 0$ band of H_3^+ with individual line positions ranging from 3.531 to 3.543 μm. The broader 3.41-μm band is due to three separate blends, R(5), centred on 3.385 μm, another R(3) blend at 3.420 μm and R(4) at 3.455 μm, comprising nine lines in all.

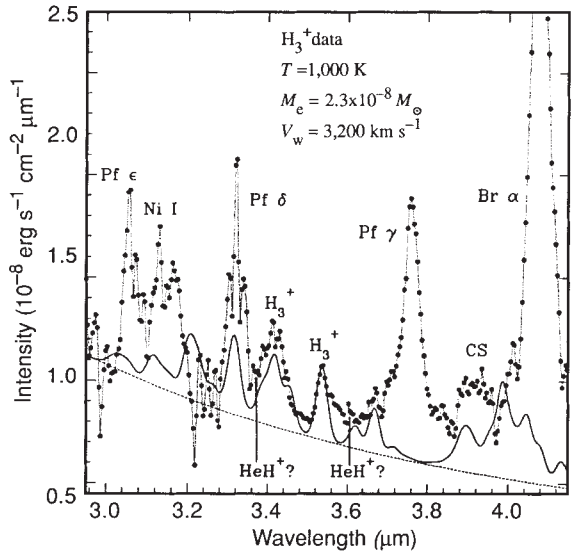

FIG. 2 Propagation of the fitted H_3^+ spectrum (solid curve) through the L window data for day 192 (filled circles) assuming T_{exc} = 1,000 K. The dashed curve represents the continuum background. Assignments other than H_3^+ and HeH^+ are from ref. 6.

exists of hydrogen in the excited $n = 2$ and $n = 3$ states. These excited states contribute considerably to the formation of H_2^+. The process

$$H(n=2) + H \rightarrow H_2^+ + e \quad (3)$$

which has a threshold of 0.75 eV is a principal formation mechanism in hot stellar winds (J. M. C. Rawlings, J. E. Drew & M. J. Barlow, manuscript in preparation). The process

$$H(n=3) + H \rightarrow H_2^+ + e \quad (4)$$

is exothermic and together with reaction (3) is an important source of molecules in the supernova.

The presence of helium enhances the formation of H_2^+ and H_2, and through the reaction[14]

$$He^+ + H \rightarrow HeH^+ + h\nu \quad (5)$$

leads to a significant abundance of HeH^+.

In calculating the molecular abundances in the envelope gas, we have adopted the rate constants and physical conditions used by Xu *et al.*[13] in modelling the hydrogen recombination spectra. They assumed a temperature of 3,000 K for the gas. At this temperature associative ionization, reaction (3), is the chief source of H_2^+ and ultimately H_3^+. The $n = 2$ level is populated by collisions from energetic electrons and by recombinations, and removed by two-photon decay, collisions with thermal electrons and ionization by continuum photons. Ionization from $n = 2$ is important in the ionization balance of the hydrogen gas.

The abundance of H_3^+ depends critically on the rate coefficients of associative ionization, reactions (3) and (4), and of dissociative recombination

$$H_3^+ + e \rightarrow H + H + H \quad (6)$$

$$\rightarrow H_2 + H \quad (7)$$

about which there is considerable uncertainty[15]. The calculated abundances are correspondingly uncertain. If we assume reactions (3), (4), (6) and (7) are all fast[15], the chemical model yields the abundances of H_3^+ and HeH^+ given in Table 1 for various times. The H_3^+ mass at day 200 is in reasonable agreement with that deduced from the spectrum at day 192. Had we assumed that the dissociative recombination rates were slow[16], however, the model would have produced an H_3^+ mass around $10^{-5}\ M_\odot$, far more than the observed spectrum could accomodate.

Also shown in Table 1 is the mass of HeH^+ as a function of time, showing that the model produces ~40 times as much H_3^+ as HeH^+ by number. There exist in the spectra weak features which may correspond to the HeH^+ vibrational transitions at 3.364 μm and 3.607 μm.

The L-window spectra of ref. 6 at days other than day 192 do not provide data of sufficient quality to enable us to carry out detailed spectroscopic fitting. In Table 2, however, we compare the intensities of the 3.53-μm feature with those of H I Brackett α and Pfund γ as measured by Meikle *et al.*[6]. The 3.53-μm emission seems to track these recombination lines, as expected from the chemical scheme outlined above, lending further weight to our identification of H_3^+.

We conclude that our fit of H_3^+ to the supernova data for day 192 produces a spectral profile consistent with that observed. It requires a mass of $\sim 10^{-7}\ M_\odot$, which can be produced by a plausible chemical model. The high abundance of H_3^+ shows that minimal microscopic mixing of the heavy elements has taken place, as they would prevent the formation of H_3^+ by destroying H_2 in endothermic reactions. The existence of H_3^+ places an upper limit of ~3,000 K on the temperature of the envelope, a temperature which must be achieved in the absence of heavy elements as cooling agents. Although a sodium doublet may contribute to the 3.41-μm emission, the features at 3.53, 3.36 and 3.61 μm were unassigned previously. We believe that the observational and theoretical evidence strongly supports the presence of H_3^+ in SN1987A and weakly supports the presence of HeH^+. If correct, we have now identified H_3^+ beyond the Solar System and also identified extraterrestrial HeH^+. □

TABLE 2 Comparison of 3.53-μm intensity with H I Br α and Pf γ

Epoch (days)	3.53 μm	Br α	Pf γ
110	2.2	18.5	6.5
192	1.0	16.0	5.5
255	0.35	7.4	2.5
285	0.30	—	2.4
349	0.17	5.9	1.0

Units: 10^{-10} erg s^{-1} cm^{-2}.

Received 17 July; accepted 8 November 1991.

1. Suzuki, H. *Prog. theor. Phys.* **62,** 936-947 (1979).
2. Herbst, E. & Klemperer, W. *Astrophys. J.* **185,** 505-513 (1973).
3. Geballe, T. R. & Oka, T. *Astrophys. J.* **342,** 855-859 (1989).
4. Black, J. H., van Dishoeck, E. F. & Woods, R. C. *Astrophys. J.* **358,** 459-467 (1990).
5. Drossart, P. *et al. Nature* **340,** 539-541 (1989).
6. Meikle, W. P. S., Allen, D. A., Spyromilio, J. & Varani, G.-F. *Mon. Not. R. astr. Soc.* **238,** 193-223 (1989).
7. Oka, T. & Geballe, T. R. *Astrophys. J.* **351,** L53-56 (1990).
8. Maillard, J.-P., Drossart, P., Watson, J. K. G., Kim, S. J. & Caldwell, J. *Astrophys. J.* **363,** L37-40 (1990).
9. Miller, S. & Tennyson, J. *Astrophys. J.* **335,** 486-490 (1988).
10. Kao, L., Oka, T., Miller, S. & Tennyson, J. *Astrophys. J. Suppl.* **77,** 317-329 (1991).
11. Lucy, L. B., Danziger, I. J. & Gouiffes, C. *Astr. Astrophys.* **243,** 223-229 (1991).
12. Phillips, M. M. & Williams, R. E. in *Supernovae* (ed. Woosley, S. E.) 36 (Springer, New York, 1991).
13. Xu, Y., McCray, R., Oliva, E. & Randich, S. *Astrophys. J.* (in the press).

14. Lepp, S., Dalgarno, A. & McCray, R. *Astrophys. J.* **358,** 262–267 (1990).
15. Amano, T. *Astrophys. J.* **329,** L121–124 (1988).
16. Adams, N. G. & Smith, D. in *Astrochemistry* (ed. Vardya, M. S. & Tarafdar, S. P.) 1 (Reidel, Dordrecht, 1986).

ACKNOWLEDGEMENTS. We acknowledge the assistance of P. Meikle in the preparation of this paper, and thank him and R. Cummings for the latest processed data. We also thank D. Allen and H. Schild for discussions. J.T. and S.M. acknowledge support from the SERC. A.D. and S.L. acknowledge support from the NSF, Division of Astronomical Sciences.

Observation of gradual brightening of P Cygni due to stellar evolution

Mart J. H. de Groot* & Henny J. G. L. M. Lamers†

* Armagh Observatory, College Hill, Armagh BT61 9DG, Northern Ireland
† Astronomical Institute and SRON Laboratory for Space Research, Sorbonnelaan2, 3584 CA, Utrecht, The Netherlands

WITH the exception of supernova outbursts, or changes in the pulsational periods of Cepheid variables arising from their changing internal structure, the evolution of stars is generally much too slow to have been detected during the era of modern astronomy. A few stars, such as the red supergiants ρ Cas and RW Cep, have shown spectral changes on a timescale of decades which have been attributed to evolutionary effects[1], but these changes are mostly erratic and the evolutionary interpretation is uncertain. Here we report an analysis of modern and historical (back to about AD 1700) photometric measurements of the star P Cygni. We find a steady change of apparent brightness, and argue that it is due to evolution of the star. The change is about twice as fast as standard models predict, but the difference may be due to mis-estimation of the star's mass or inadequate treatment of atmospheric expansion in the stellar models.

P Cygni (HD193237) is a luminous blue variable of spectral type B1 Ia+ with a present mean visual brightness of 4.8 mag. Its effective temperature is $T_{\rm eff} = 19{,}300 \pm 700$ K, and its luminosity, L, is given by $\log L/L_\odot = 5.86 \pm 0.10$ (ref. 2). A comparison of these values with predicted evolutionary tracks[3] suggests an initial mass of $50 \pm 10 M_\odot$ and a present mass of $30 \pm 10\ M_\odot$.

P Cyg's photometric history has been recorded in several bibliographies[4–6]. Mueller and Hartwig's list is a careful interpretation of the many historical observations of P Cyg with the stellar magnitude estimates reduced to the system of the Potsdam Durchmusterung. We have transformed these photometric magnitudes into the V-magnitude scale to couple the historical and modern observations into one system.

Measurements of the visual magnitudes of P Cyg between 1700 and 1990 are listed in Table 1. The eighteenth- and nineteenth-century magnitudes of P Cyg are based on optical estimates through small telescopes by many observers. The accuracy of the individual observations is estimated to be ~0.3 mag. Apart from this observational uncertainty, there is the irregular intrinsic brightness variation of P Cyg. This is assumed to be the same as the modern brightness variations in V of 0.2 mag (ref. 7). We have averaged the magnitude estimates of the eighteenth- and nineteenth-century over periods of between 8 and 29 years, depending on the frequency of the observations at each epoch. This has the advantage that it produces a long-term light curve essentially free from the rapid variations, and it eliminates as far as possible the small differences between individual observers.

The observations between 1898 and 1917 contain the first photoelectric photometry of P Cyg, with the magnitudes transformed to the standard system by Mueller and Hartwig[4]. Between 1920 and 1950, observers used a variety of photoelectric detectors and almost any combination of filters, until the international UBV system was established in 1953. Therefore we have not tried to reduce observations in this period to the scale of the V-magnitude. The mean value of the unspecified number of photometric observations of P Cyg between 1952 and 1954 by Hiltner[8] in the UBV-systems is listed under epoch 1953. The magnitude at epoch 1966 is the mean of only two observations of P Cygni in 1965 and 1966 with the very accurate 13-colour system of Johnson and Mitchell[9]. The magnitude in their (52)-filter (centred at 520 nm) was converted to the V-magnitude by means of the transformation formula of ref. 10. Percy and Welch[11] observed the star on 11 nights in 1982. The visual magnitude at epoch 1988 is derived from the photoelectric measurements by members of the American Association of Variable Star Observers between 1985 and 1990 (ref. 12).

The mean visual magnitudes are plotted in Fig. 1, which clearly shows the trend of the increasing visual brightness. The weighted least-square fit through the data is

$$V = 5.24 - (1.54 \pm 0.20) \times 10^{-3}(t - 1700) \qquad (1)$$

where t is the date in years, which corresponds to a brightening of $\mathrm{d}V/\mathrm{d}t = -0.15 \pm 0.02$ mag per century.

The theory of evolution of massive stars predicts that the evolution occurs at almost constant L throughout most of the star's life. This is because massive stars do not have degenerate cores and because the energy transport is mainly by radiation, except in the red-supergiant phase. A constant luminosity implies that the changes in V are due to the redistribution of the emitted radiation over the spectrum: a change in V reflects the change in the star's bolometric correction (BC) and $T_{\rm eff}$. A change in $T_{\rm eff}$ is related to a change in V according to

$$\frac{\mathrm{d}\log(T_{\rm eff})}{\mathrm{d}t} = \frac{\mathrm{d}\log(T_{\rm eff})}{\mathrm{d(BC)}} \frac{\mathrm{d(BC)}}{\mathrm{d}t} = -0.027 \pm 0.004 \qquad (2)$$

in mag per century. We adopted the empirical relation between BC and $T_{\rm eff}$ for supergiants of luminosity class Ia, tabulated by Schmidt-Kaler[13], which gives $\mathrm{d(BC)}/\mathrm{d}\log(T_{\rm eff}) = -5.63$ mag near $T_{\rm eff} \approx 20{,}000$ K. The observed gradual brightening of P Cyg thus implies a steady decrease in $T_{\rm eff}$ of $6 \pm 1\%$ per century. The decrease in $T_{\rm eff}$ is related to an increase in radius because $L \sim R_*^2\ T_{\rm eff}^4$ is constant. The timescale $\tau(R_*)$ in which R_* increases by a factor e is 320 ± 60 yr.

The location of P Cyg in the Hertzsprung–Russell diagram (HRD) is shown in Fig. 2, which also shows some predicted evolutionary tracks of massive stars with mass loss and convective overshooting[3]. P Cyg lies in a region of the HRD that is crossed twice during the evolution of a massive star. The first crossing occurs immediately after the main-sequence phase when the energy of the star is generated by a hydrogen-burning shell and by contraction of the core. The outer layers react by

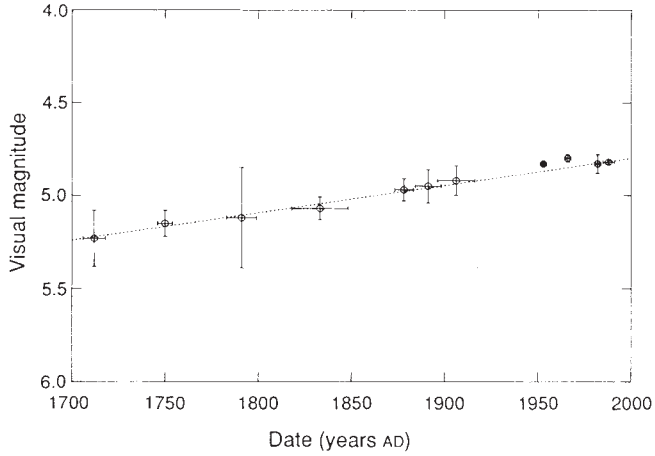

FIG. 1 Visual magnitude of P Cyg as a function of time. Dotted line, least-square fit given by equation (1) which shows the gradual photometric brightening of 0.15 ± 0.02 mag per century.